HHS Public Access

Author manuscript

Nat Biotechnol. Author manuscript; available in PMC 2014 July 17.

Published in final edited form as:

Nat Biotechnol. 2014 January ; 32(1): 84–91. doi:10.1038/nbt.2754.

Highly efficient generation of airway and lung epithelial cells from human pluripotent stem cells

Sarah X.L. Huang[1,2], **Mohammad Naimul Islam**[2], **John O'Neill**[3], **Zheng Hu**[1], **Yong-Guang Yang**[1,2], **Ya-Wen Chen**[1,2], **Melanie Mumau**[1,2], **Michael D. Green**[1], **Gordana Vunjak-Novakovic**[2,3], **Jahar Bhattacharya**[2,5], and **Hans-Willem Snoeck**[1,2,4]

[1]Columbia Center for Translational Immunology, Columbia University Medical Center, New York, NY, USA

[2]Department of Medicine, Columbia University Medical Center, New York, NY, USA

[3]Department of Biomedical Engineering, Columbia University, New York, NY, USA

[4]Department of Microbiology and Immunology, Columbia University Medical Center, New York, NY, USA

[5]Department of Physiology & Cellular Biophysics, Columbia University Medical Center, New York, NY, USA

Abstract

The ability to generate lung and airway epithelial cells from human pluripotent stem cells (hPSCs) would have applications in regenerative medicine, drug screening and modeling of lung disease, and studies of human lung development. We established, based on developmental paradigms, a highly efficient method for directed differentiation of hPSCs into lung and airway epithelial cells. Long-term differentiation *in vivo* and *in vitro* yielded basal, goblet, Clara, ciliated, type I and type II alveolar epithelial cells. Type II alveolar epithelial cells generated were capable of surfactant protein-B uptake and stimulated surfactant release, providing evidence of specific function. Inhibiting or removing agonists to signaling pathways critical for early lung development in the mouse—retinoic acid, Wnt and BMP—recapitulated defects in corresponding genetic mouse knockouts. The capability of this protocol to generate most cell types of the respiratory system suggests its utility for deriving patient-specific therapeutic cells.

The capacity to generate lung and airway epithelial cells from human pluripotent stem cells (either embryonic stem (ES) or induced pluripotent state (iPS) cells) would have multiple applications. These include the recellularization of decellularized lung scaffolds to provide

Correspondence: Hans-Willem Snoeck, MD, PhD, Columbia Center for Translational Immunology, Columbia University Medical Center, Black Building, 630W168th Str, Rm 1501E, New York, NY 10032, Phone: 212 342 0182, hs2680@columbia.edu USA.

Author contributions:

SXLH performed most experiments, developed this protocol and co-wrote the manuscript; NMI performed functional analysis of ATII cells supervised by JB; MM, MDG and YWC gave technical advice and assisted SXLH experimentally; ZH performed kidney capsule transplantations supervised by YGG; JON provided human lung ECM and these experiments were supervised by GVN; HWS developed the concept, co-analyzed primary data and co-wrote the manuscript with SXLH

an autologous graft for transplantation, the study of human lung development, modeling of diseases that primarily affect airway epithelial cells, and drug screening[1].

Trachea and bronchi are lined by a pseudostratified epithelium. The alveoli consist of alveolar epithelial type I (ATI) cells, which are essential for gas exchange, and alveolar epithelial type I (ATII) cells, which produce surfactant, critical for the maintenance of alveolar integrity[2]. The respiratory system is derived from lung buds on the anterior ventral aspect of the definitive endoderm (DE), which grow and branch in a stereotyped pattern driven by renewing progenitors on the tips[3, 4]. Directed differentiation of PSCs into pulmonary tissue should therefore proceed by first differentiating into DE, followed by ventral anterior foregut endoderm (AFE) and specification of lung and airway lineages.

We have previously demonstrated that AFE can be generated from hPSCs by exposing Activin A-induced DE to dual TGF-β and BMP inhibition[5]. The AFE OK cells could be partially specified towards a putative lung bud fate, as suggested by expression of NKX2.1. However, purity of $NKX2.1^+FOXA2^+$ cells was <40%, and expression of specific markers of lung and airway epithelial cells was not detected. A recent report described differentiation of hPSCs to lung progenitors at low efficiency; only a few percent of $NKX2.1^+p63^+$ putative airway progenitors were obtained, and the cells did not express markers of mature airway epithelial cells[6]. In mouse studies[7], a NKX2.1:GFP reporter ES line was used to isolate $NKX2.1^+$ cells after differentiation into AFE by a strategy very similar to our previously published protocol[5]. The cells were committed to a lung and thyroid fate, and amenable to further differentiation, although expression of markers of ATI and ATII cells remained sporadic[7]. Wong *et al.*[8] showed differentiation of hPSCs into cystic fibrosis transmembrane conductance regulator (CFTR)-expressing proximal airway cells. However, the efficiency of this protocol is unclear, and the generation of distal lung epithelial cells was not documented at the protein or functional level.

Here we describe strategies to achieve high yields of developmental lung progenitor cells, and for their differentiation *in vivo and in vitro* into functional respiratory epithelial cells. The cells express markers of at least six types of lung and airway epithelial lineages and were particularly enriched in distal ATII cells capable of surfactant protein-B (SP-B) uptake and release. Notably, a high degree of similarity was observed between *in vitro*–differentiated hPSC-derived cells and cultured fetal human lung (FHL), and between *in vivo* differentiated hPSC-derived lung field cells and adult human lung (AHL).

Results

Induction of highly enriched $FOXA2^+NKX2.1^+$ lung and airway progenitors

We have previously shown that DE, induced using established protocols[9–12], can generate AFE ($FOXA2^+SOX2^+CDX2^-$) following inhibition of BMP and TGF-β signaling[5]. Application of a ‘ventralization cocktail’ containing WNT, FGF10, KGF, BMP4 and RA[13–17,18]—factors involved in dorsoventral patterning of the AFE and lung bud specification— yielded cultures containing $NKX2.1^+FOXA2^+$ cells that corresponded to the lung field of the AFE[5]. The enrichment in $NKX2.1^+FOXA2^+$ cells never exceeded 35–40%, however, and specific lung and airway epithelial cell markers were absent.

To improve lung field specification efficiency from AFE we first refined the AFE induction approach. In the mouse embryo, DE cells fated to become AFE pass through a zone where the Nodal/Activin inhibitor Lefty and the BMP4 inhibitor Noggin are expressed[19, 20], likely explaining why blocking TGF-β and BMP signaling is required for AFE specification. Subsequently, the cells are exposed to the Wnt inhibitor, Dkk1[21]. Indeed, sequential inhibition of these pathways after DE induction yielded efficient lung field induction. Cells were first exposed to small-molecule inhibitors of signaling by BMP (dorsomorphin (DSM)[22]), TGF-β(SB431542 (SB)[23]) and WNT (IWP2 (I) that inhibits endogenously produced Wnts by blocking porcupine-mediated Wnt palmitoylation[24]). The cells were then cultured until d15 in the presence of the ventralization factors CHIR99021 (a small molecule GSK inhibitor that mimics WNT signaling)[25], FGF10, KGF, BMP4 and RA (CFKB+RA) (Fig. 1a). Compared to continuous supplementation of DSM/SB only, supplementation of DSM/SB from d4.5 to 5.5 followed by SB/I from d5.5 to d6.5 significantly increased the fraction of $NKX2.1^{+}FOXA2^{+}$ cells (from 51.2±1.6 to 70.1±1.2 %, P = 0.004, n = 3) and of *NKX2.1* mRNA (Fig. 1a) at d15. Reversing the DSM/SB->SB/I sequence to SB/I->DSM/SB or using SB/I alone was detrimental for NKX2.1 protein expression (22.0 ±4.8% and 18.8±5.0% $NKX2.1^{+}FOXA2^{+}$ cells, respectively) and mRNA expression (Fig. 1a). These data suggest that prepatterning occurs during AFE development.

We further modified this protocol by optimizing timing of dissociation of DE (d4, Fig. S1a) and the concentration of RA in the 'ventralization' stage (50–100 nM, Fig. S1b). These manipulations resulted in cultures where 95.7±3.2% of the cells were $FOXA2^{+}$ and 86.4±1.7% were $FOXA2^{+}NKX2.1^{+}$ (n = 3, ten 10x fields quantified per experiment) (Fig. 1b,c). Expression of NKX2.1 mRNA was 3,170±120-fold higher compared to liver-specified cells, and more than 60,000-fold higher than in DE (d4 in our protocol). However, the efficiency of lung progenitor induction was lower in two iPS lines generated by Sendai virus[26] (sviPSC, $FOXA2^{+}$: 87.3±4.4%, $FOXA2^{+}NKX2.1^{+}$: 37.0±1.6%) and mRNA transfection[27] (mRNAiPSC, $FOXA2^{+}$ 69±2.7%, $NKX2.1^{+}FOXA2^{+}$ 36.1±4.3 %), respectively (Fig. S2). Notably, the optimal DE dissociation time point in both iPS lines was d4.5 to d5 (not shown).

At d15 of the culture, no markers of mature lung or airway epithelial cells were detected by immunofluorescence (Fig. S3a, positive staining controls using AHL, Fig. S3b). Furthermore, qPCR (Fig. S4) or immunofluorescence (not shown) evidence for differentiation into the thyroid (PAX8, TG, TSHR), which also expresses NKX2.1[7, 28], was absent. However, other types of contaminating cells were present, and these varied depending on the cell lines used. In RUES2 cells, clusters of $FOXA2^{bright}NKX2.1^{-}$ cells that stained weakly for the neural marker TUJ1 (Fig. 1d, arrows), but not for PAX6 (not shown) were observed, a phenotype suggestive of midbrain floorplate neuronal precursors[29]. Cultures of RUES2 cells (Fig. 1e) and sviPSCs (not shown) also contained islands of cells that were negative for NKX2.1, FOXA2, (Fig. 1e, arrows), SOX2, TUJ1 and PAX6 (not shown), but expressed the epithelial markers p63 (Fig. 1e, arrows) and EPCAM (not shown). Their identity is unknown. In the mRNA iPSCs, contamination with $PAX6^{+}$ neuronal cells was observed (not shown).

We next examined which factors in the 'ventralization' cocktail were essential. Removing BMP4 or WNT agonists reduced the numbers of NKX2.1$^+$ cells, while blocking these pathways or removing RA (Fig. S1b) virtually abolished the generation of these cells (Fig. 2). These data are consistent with mouse genetic models, where BMP on one hand and RA and Wnt signaling on the other hand have non-redundant roles in dorsoventral patterning of the AFE and lung bud specification, respectively [13, 18, 30, 1617]. However, removing either FGF10 (Fig. 2), FGF7 (Fig. 2) or both (not shown), or inhibition of FGF signaling (not shown) had no effect, suggesting that FGF signaling is, in contrast to the mouse, dispensable in the human system.

Differentiation of NKX2.1$^+$FOXA2$^+$ cells *in vivo*

To determine the *in vivo* differentiation potential of these NKX2.1$^+$FOXA2$^+$ cells, we transplanted 10^6 d15 RUES2 cells under the kidney capsule of immunodeficient NSG mice. After 6 months, we observed multiple macroscopic growths, which contained cystic and tubular structures (Fig. 3a) lined by a uniformly FOXA2$^+$SOX2$^+$NKX2.1$^+$(Fig. 3b) epithelium that ranged from pseudostratified containing cells consistent with basal, ciliated, Clara and goblet cells to a monolayer consisting of flatter cells (Fig. 3a). Glandular structures resembling submucosal glands were also present (Fig. 3a).

All tested markers of mature lung and airway epithelial cells were detected. These included mucins (MUC1, MUC5AC, MUC2; goblet cells), FOXJ1 (ciliated cells), CC10 (Clara cells), p63 and NGFR (basal cells) [31], pro-SP-C, SP-C and SP-B (ATII cells) as well as AQP5, HOPX and PDN (ATI cells) (Fig. 3b). These staining patterns were remarkably similar to those observed in FHL (Fig. S5) and AHL (Fig. S3b). The structures were surrounded by smooth muscle and cartilage, in addition to areas containing looser connective tissue (Fig. 3a). All cells, including the mesodermal cells, were of human origin, as determined by staining with antibodies specific for human nuclei (Fig. S6).

Together, these data indicate that d15 cells in our protocol almost exclusively give rise *in vivo* to lung and airway endoderm, in addition to mesodermal cells that adopt cell fates consistent with the mesodermal elements surrounding trachea and large airway.

Differentiation of NKX2.1$^+$FOXA2$^+$ cells *in vitro*

BMP4, FGF10, KGF, Wnt, and RA are involved in the differentiation of respiratory epithelium[13–15, 17, 32–36]. However, upon initiation of branching morphogenesis in mouse embryos, RA signaling inhibits distal lung and favors proximal airway development[3635]. We have shown that removal of BMP4, the role of which is controversial and model-dependent[16, 32], from the growth factor cocktail increased the expression of *SFTPC* (SP-C) mRNA, though pro-SP-C protein was not detected[5]. Therefore, we focused subsequent experiments mostly on cells cultured in the presence of Wnt agonism (CHIR), FGF10 and KGF (CFK).

D15 lung-specified AFE cells were replated after mild trypsinization, brief sedimentation, and collection of larger cell clumps for replating (Fig. 4a). Preliminary experiments indicated that these were depleted of P63$^+$FOXA2$^-$NKX2.1$^-$ cells and of most neural

elements, which were present in smaller aggregates in the supernatant(not shown). In these cultures, cells grew as large colonies that were virtually entirely positive for FOXA2 (not shown), NKX2.1 and SOX2 at day 25 (Fig. 4b,c), and contained $p63^{+}NKX2.1^{+}$ cells at the periphery (Fig. 4b,d). In sviPSCs, 86.8±2.2% of the cells were $FOXA2^{+}$ and 75.2±2.9% were $FOXA2^{+}NKX2.1^{+}$, while in our mRNAiPSCs 88.5±1.0% of the cells were $FOXA2^{+}$ and 79.1±1.7% were $FOXA2^{+}NKX2.1^{+}$ (Fig. S2). In both iPSC lines, but not in RUES2 cells, contaminating neuronal cells were observed. Notably, whereas these were $TUJ1^{+}PAX6^{-}$ in sviPCs, a significant number of $PAX6^{+}$ cells were observed in the mRNA iPSCs (Fig. S2).

Except for sporadic expression of MUC5AC (Fig. 4d), other markers of respiratory epithelial cells were absent at d25 (not shown). At d48, however, expression of all markers detected in growths arising after transplantation in NSG mice were observed (Fig. 5a,b; whole-culture tile scans shown in Fig. 5c and Fig. S7; data from sviPSCs shown in Fig. S8). In addition, we noticed that staining for the secreted mucins (MUC5AC (not shown), MUC2 and MUC5B, Fig. S9) and CC10 (Fig. S9), extended outside cell boundaries as defined by EPCAM expression, and occurred in structures that were discernable in bright field. These findings suggest secretory activity of both goblet and Clara cells. The cells positive for PDN and AQP5 displayed flat, crescent-shape nuclei at the periphery of the cells (Fig. 5b, insets), a morphology typical of ATI cells, while SP-B expression occurred in a punctate pattern, suggestive of lamellar bodies of ATII cells where surfactant accumulates (Fig. 5b, inset).

Next, we examined the effect of adding dexamethasone, 8-bromo-cAMP and isobutylmethylxanthine (DCI) (Fig. 5a,c), factors that induce alveolar maturation in fetal mouse lung explants and enhance surfactant protein expression in mES-derived lung progenitors [7, 37]. In the presence of DCI, $SP\text{-}B^{+}$ cells became the predominant cell type (Fig. 5c). Furthermore, only under these conditions was expression of mature SP-C detected, although at a much lower frequency than SP-B, (Fig. 5c). More than 50% of the cells expressed SP-B, while the frequency of all other cell types ranged between 2 and 5 % (n=3). It has been shown in fetal rat lung explant cultures that SP-C expression is more highly responsive to mechanical stretch than SP-B expression[38], consistent with the lower SP-C expression in cultured cells. Addition of DCI at d15 did not result in SP-B expression at d25 however (not shown). Most likely, the cells respond to DCI if and when they reach a differentiation stage that allows them to respond with increased surfactant production. Cell number increased 35-fold up to d25, was similar in the presence or absence of DCI, and then plateaued (Fig. 5d). These data attest to the high efficiency of this protocol, and suggest cessation of cellular expansion coinciding with expression of lineage-specific epithelial markers.

As hPSCs-derived cells are cultured on fibronectin-coated plastic, marker protein expression and cell morphology may differ from that observed in native lung tissue. Therefore, we cultured dissociated cultured FHL under the same conditions (CHIR, FGF7, FGF10 and DCI) for three weeks. Both by immunofluoresence (Fig. S10a) and by transmission electron microscopy (TEM) (Fig. 6a) cultured FHL was very similar to differentiated hESCs. Notably, whereas in AHL (Fig. S10b) and in d15 differentiated ESCs 6 months after grafting under the kidney capsule of NSG mice (Fig. 3b), $p63^{+}$ cells expressed NGFR, a marker of

basal cells[31], p63$^+$ cells in native and in cultured FHL and in hPSCs differentiated *in vitro* (Fig. S10b) did not co-express NGFR. These findings suggest that NGFR expression on basal cells is developmentally regulated, and that hPSCs differentiated *in vitro* are more similar to FHL than to AHL. TEM showed structures consistent with lamellar bodies of ATII cells and with multivesicular bodies, precursors of lamellar bodies, in both FHL and differentiated hPSCs (Fig. 6a). Together, these findings show that hPSCs differentiated into lung and airway are nearly indistinguishable from cultured FHL.

To assess the function of the SP-B expressing cells, we examined their capacity to take up surfactant proteins, a distinguishing feature of ATII cells[39]. By flow cytometry, only 0.6±0.1 % of the cells showed detectable uptake of fluorescent BODIPY-labeled recombinant human SP-B at d15, whereas at d48 17±10% and 52±6% showed uptake in the absence and presence of DCI ($P = 0.04$, $n = 3$), respectively (Fig. 6b). The fact that functional ATII cells could be detected by flow cytometry also allows their further purification from the cultures. Next, we monitored release of BODIPY-SP-B from the cells after addition of a cell-permeable analog of diacylglycerol (DAG), a surfactant secretagogue[40]. Addition of DAG caused a rapid decrease in BODIPY-SPB fluorescence, indicative of increased release (Fig. S11). Together, these data indicate that the ATII cells generated in our cultures are functional, and that their maturation is enhanced by DCI.

We also cultured the cells from d15 on in the presence of decellularized slices of human lung. Initially, NKX2.1$^+$p63$^+$ cells were seen to be adhering to the matrix (Fig. 6ci,ii). Subsequently, cells overgrew the matrix slices and showed positive staining for SP-B (Fig. 6ciii, iv) and uptake of BODIPY-SP-B at d48 (Fig. 6c,v). The morphology of the BODIPY SP-B$^+$ cells was very similar to that seen using two-photon microscopy after uptake of BODIPY-SP-B in live mouse lung (Fig. 6vi). These data show the ability of the NKX2.1$^+$p63$^+$ cells to attach to native lung matrix, grow and express distinct functional properties of pulmonary cells, an important feature for potential applications in which lung progenitors are used to treat lung disease.

Finally, we confirmed our protein expression data by qPCR, using DE and DE differentiated into the hepatic lineage[41] as controls (Fig. 6d). We observed early induction of mRNAs for distal markers without protein expression at d15, when no protein expression is detected. These mRNAs subsequently disappear, and then re-appear as the cells mature, this time accompanied by ample protein expression. It is possible that upon initial lung specification, several lung specific genes are temporarily de-repressed, and subsequently controlled in a lineage-specific fashion. Differentiation on human lung matrix or on plastic coated with fibronectin was similar in terms of mRNA expression of lung and airway markers. Furthermore, these experiments also confirmed that better distal lung differentiation is achieved in the absence of BMP4 and RA after lung field induction.

Discussion

We report differentiation of hPSCs into lung field progenitors that can differentiate into at least six identifiable types of lung and airway cells *in vivo* and *in vitro.* Notably, a high degree of similarity was observed between *in vitro*–differentiated hPSC-derived cells and

cultured FHL, and between *in vivo* differentiated hPSC-derived lung field cells and AHL. The only endodermal cells detected after transplantation in NSG mice were lung and airway epithelial cells. However, a large mesodermal component consisting of smooth muscle, cartilage, and loose connective tissues was present, despite the very high enrichment of lung field endoderm in the transplanted cells. These cells likely originated from small amounts of contaminating mesoderm. The fact that these mesodermal cells appeared to differentiate into the appropriate mesodermal elements surrounding the airways may suggest that pulmonary endoderm has an instructive role in the development of appropriate mesodermal elements in this model.

The efficiency of our differentiation protocol and the nature of contaminating lineages varied across hPSC lines, a reflection of the well-documented variability in the lineage-specific differentiation potential of ES[42] and iPS[43, 44] lines. Among the ES lines tested (RUES1, RUES2, H1, H9, HES2), HES2 and RUES2 were most efficient in OK AFE induction. We focused on RUES2, as it is NIH-approved. Furthermore, morphogen concentration and timing of culture stages may require optimization for each individual line. This notion is supported by our observation that the optimal timing of DE dissociation is line-dependent and by the observation that ES lines are heterogeneous with respect to Wnt signaling[45].

Wong *et al*.[8] generated CFTR-expressing proximal airway cells from hiPSCs by exposing DE to SHH and FGF2 to induce AFE and specifying lung progenitors by addition of FGF10, FGF7 and a low concentration of BMP4 (5 ng/ml), followed by air-liquid interphase culture. We systematically compared the AFE and lung field induction protocols[8] described in that study with ours, for the hPSC lines used here (Fig. S12). Applying the AFE induction protocol of Wong *et al*.[8] (SHH+FGF2) or ours (DSM/SB->SB/I), followed by lung field induction using the protocol of Wong *et al*.[8] yielded only sporadic NKX2.1^{+} cells. However, AFE induction using SHH and FGF2, followed by our CFKB+RA lung field induction strategy yielded >50% NKX2.1 cells (Fig. S12). Similar data were obtained using our sviPSCs (not shown). Taken together, these data confirm that Wnt, BMP4 and RA are essential for efficient induction of lung progenitors from hPSCs (Fig. 2). It is possible that the protocol reported by Wong et al.[8] is oriented more toward generation and selection of precursors of proximal airway cells in air-liquid interphase cultures, whereas our protocol generates a wider array of the respiratory epithelium that is biased towards distal cells. Clearly, the two protocols provide alternative strategies to induce AFE, suggesting that complex and hierarchical relationships between TGF-β, BMP, Wnt, SHH and FGF2 signaling in the specification of AFE from DE need to be further examined.

The ability to generate ATII cells from hPSCs will allow modeling of diseases such as congenital surfactant deficiency syndromes[39]. Furthermore, ATII cells have recently been identified as alveolar stem cells[46] and may be at the origin of lung adenocarcinoma[47]. As the current protocol yields most cell types of the respiratory system, it will allow studies of lineage determination and may help to address a central challenge in lung tissue engineering using autologous, iPSC-derived cells: generating sufficient numbers of cells with the appropriate variety and ratio of epithelial cells and their progenitors normally found in the lung.

Online Methods

Maintenance of hPSCs

RUES2 (Rockefeller University Embryonic Stem Cell Line 2, NIH approval number NIHhESC-09-0013, Registration number 0013; passage 13–24) and Sendai Virus and modified mRNA generated HDF iPS lines (derived from healthy fibroblasts, passage 12–25, purchased from the Mount Sinai Stem Cell Core facility) were cultured on mouse embryonic fibroblasts as previously described[5]. Mouse embryonic fibroblasts (GlobalStem, Rockville, MD) were plated at a density of ~25,000 cells/cm^2. hPSCs were cultured in a medium of DMEM/F12, 20% knockout serum replacement [Gibco (Life Technologies, Grand Island, NY)], 0.1 mM β-mercaptoethanol (Sigma-Aldrich, St. Louis, MO), and 20 ng/ml FGF-2 (R&D Systems, Minneapolis, MN). Medium was changed daily and cells were passaged with accutase/EDTA (Innovative Cell Technologies, San Diego, CA) every 4 days at 1:24 dilution. Cultures were maintained in undifferentiated state in a 5% CO_2/air environment. hPSC differentiations were maintained in a 5% CO_2/5% O_2/95% N2 environment unless indicated elsewhere.

Induction of endoderm

24 hour primitive streak formation and 3–4 days of endoderm induction were performed in serum-free differentiation (SFD) media of DMEM/F12 (3:1) (Life Technologies) supplemented with N2 [Gibco (Life Technologies)], B27 (Gibco), ascorbic acid (50 μg/ml, Sigma), Glutamax (2 mM, Life Technologies), monothioglycerol (0.4 μM, Sigma), 0.05% bovine serum albumin (BSA) (Life Technologies), 1% penicillin-streptomycin (Thermo Fisher Scientific, Waltham, MA), as previously described with slight modification[5]. hPSCs were treated with Acutase (2 min at 37°C) and plated onto Matrigel (Life Technologies) coated 10cm tissue culture dish (1:2 dilution) for 12–24 hr to deplete residual mouse embryonic fibroblasts. Cells were then briefly trypsinized (0.05%, 1 min at 37°C) into 3–10 small cell clumps and plated onto low attachment 6-well plates [Costar (Corning Incorporated, Tewksbury MA)] (1:1 dilution) to form embryoid bodies in serum free differentiation media. For primitive streak formation, Y-27632, 10 μM [Tocris (R&D Systems)] and human BMP4, 3ng/ml were added in the media for 24 hr. Embryoid bodies were then collected, resuspended in endoderm induction media containing Y-27632, 10 μM, human BMP4, 0.5ng/ml; human bFGF, 2.5 ng/ml (R&D Systems); human activin A, 100 ng/ml (R&D Systems) for 72, 84, or 96 hr on low-adherence plates. Cells were fed every 36–48 hr (depending on the density) by removing half of the old media and adding half fresh media.

Induction of anterior foregut endoderm

On day 4, 4.5 or 5, embryoid bodies were dissociated into single cells using 0.05% Trypsin/EDTA [cellgro (Corning)] (2–4 min). For anterior foregut endoderm induction, endodermal cells were plated on fibronectin-coated (Sigma) 48-well tissue culture plates (~70,000–100,000 cells/well) in serum-free differentiation media supplemented with 1.5μM Dorsomorphin dihydrochloride (Tocris, R&D) and 10 μM SB431542 [Tocris (R&D Systems)] for 24hr, and then switched to 24hr of 10 μM SB431542 (Sigma) and 1 μM IWP2 [Tocris (R&D Systems)] treatment. In some experiments, the AFE were specified by 48 hr

of Dorsomorphin (1.5μM) and SB431542 (10 μM) treatment only, without switching to SB431542 and IWP2. Hepatic conditions contain BMP-4, 50 ng/ml; HGF, 10 ng/ml; dexamethasone, 40 ng/ml; bFGF, 10 ng/ml; VEGF, 10 ng/ml; TGFα, 20 ng/ml; murine EGF, 20 ng/ml (All from R&D, except dexamethasone from Sigma)[5, 41].

Induction of lung progenitors

For d6-15 lung progenitor induction, the resulted AFE were treated with a 'ventralization' cocktail containing CHIR99021, 3μM (WNT signaling agonist), human FGF10, 10 ng/ml; human FGF7, 10 ng/ml; human BMP4, 10 ng/ml; murine EGF, 20 ng/ml (optional) and all-trans retinoic acid (ATRA), 0–1 μM (all from R&D, except CHIR99021 from (Stemgent, Cambridge, MA) and ATRA from Sigma) in SFD media for 8–10 days. For RUES2 differentiation, the d8-15 cultures were maintained in a 5% CO2/air environment. For SViPS differentiation, the d12-15 cultures were maintained in a 5% CO2/air environment. In some experiments, each of the factors was withdrawn from the 'ventralization' cocktail (i.e., CHIR99021, FGF10, FGF7, BMP4 and EGF), or blocked by specific inhibitors (i.e., NOGGIN as biological inhibitor of BMP4 signaling and IWP2 as pharmacological inhibitor of WNT signaling), or added at different concentrations (i.e., RA 0, 0.05, 0.1, 0.5, 1 μM), to examine the contribution of each of the factors to the specification of lung and airway progenitors.

Induction of lung/airway epithelial maturation

On day 15/16, the lung field progenitor cells were replated after brief trypsinization onto fibronectin-coated plates at 1:5 dilution. The cells were incubated in 0.05% warm trypsin/EDTA for 1min. Trypsin was then removed by suction and wash media (IMDM+5% FCS) was added into the well, and the cell clumps were gently removed off the plate using 1ml pipet tips and transferred to a 15ml tube. After gently mixing with 1 ml pipet tips, the clumps were allowed to settle for 2 minutes. Supernatant (containing single cells and small clumps of cells (<10 cells/clump)) was removed. The remaining cell clumps were replated into fibronectin-coated plates at 1:5 dilutions in the presence of SFD containing either a combination of 5 factors (CHIR99021, 3μM; human FGF10, 10 ng/ml; human FGF7, 10 ng/ml; human BMP4, 10 ng/ml; and ATRA, 50nM), or three factors (CHIR99021, 3μM, human FGF10, 10 ng/ml; human FGF7, 10 ng/ml). D15-25 cultures were maintained in a 5% CO2/air environment. From d25 to d48, cultures were carried further in either of these two conditions with or without the addition of maturation components containing 50 nM Dexamethasone, 0.1 mM 8-Bromo-cAMP (Sigma), and 0.1 mM IBMX (3,7-Dihydro-1-methyl-3-(2-methylpro(pyl)-1*H*-purine-2,6-dione) (Sigma)[37].

Immunofluorescence Staining

Day-15, -25 or -48 cultures in 48-well tissue culture plates were fixed with 4% paraformaldehyde for 15 min at room temperature and washed twice with PBS. The cells were permeabilized in PBS with 0.25% triton and 5% fetal donkey serum (Jackson ImmunoResearch, West Grove, PA) for 15–30 min (depending on the thickness of the cultures) and blocked in 5% fetal donkey serum for 2 hr at room temperature. OCT-embedded differentiation cultures or human fetal and adult lung tissues, were sectioned into

6μM slices, put on microscopic slides, brief fixed with 95% ethanol for 2 min and further fixed with 4% paraformaldehyde for 15 min at room temperature and washed twice with PBS. The sections were permeabilized for 15min and blocked for 1hr in the solutions described above. The cell cultures and sections were stained with one, or a combination of two or three of the following primary antibodies: FOXA2/HNF-3β(goat, Santa Cruz Biotechnology, Inc., Santa Cruz, CA, Cat# sc-6554, clone M-20, 1:50), TTF-1/Nkx2.1 (mouse, Invitrogen, 18-0221, clone 8G7G3/1, 1:100), TTF-1/Nkx2.1 (Rabbit, Seven Hills Bioreagents, Cincinnati, OH, Cat# WRAB-1231, 1:1000), p63α (rabbit, Santa Cruz, sc-8344, clone H-129, 1:100), NGFR (EMD Millipore, Billerica, MA. Cat# 05-446, clone ME20.4, 1:100), Sox2 (rabbit, stemgent, 09-0024, 1:100), Sox2 (goat, Santa Cruz, Cat# sc-17320, clone Y-17, 1:100), Pax 6 (rabbit, Covance, Princeton, NJ, Cat# PRB-278P, 1:300), Pax8 (mouse, Abcam, Cambridge, MA, Cat# ab53490, 1:100), EpCAM (APC conjugated, mouse, BD Biosciences, BDB347200, 1:100), Tuj1 (mouse, Sigma, T8578, Clone 2G10, 1:4000), Mucin5AC (mouse (Biotin), Abcam, ab79082, clone 45M1, 1:100), Mucin5B (rabbit, Santa Cruz, sc-20119, clone H-300, 1:100), Mucin2 (rabbit, Santa Cruz, sc-15334, clone H-300, 1:100), Foxj1 (mouse, e-bioscience, San Diego, CA, Cat#14-9965-82, Clone: 2A5, 1:100), cc-10 (goat, Santa Cruz, sc-9770, clone C-20, 1:100), pro-SPC (rabbit, Seven Hills, WRAB-9337, 1:2000), mature-SPC (rabbit, Seven Hills, WRAB-76694, 1:1000), mature SPB (rabbit, Seven Hills, WRAB-48604, 1:1000), ABCA3 (rabbit, Seven Hills, WRAB-70565, 1:1000), Mucin1 (Armenian Hamster, NeoMarkers, Fremont, CA, Cat# HM-1630-P1ABX, clone MH1, 1:100), Podoplanin (rabbit, Santa Cruz, sc-134482, FL-162, 1:100), AQP5 (goat, Santa Cruz, sc-9890, clone G-19, 1:100), HOPX (Rabbit, Santa Cruz, sc-30216, 1:250), Anti-Nuclei Antibody (EMD Millipore, MAB1281, clone 235-1, 1:200). Secondary antibodies were donkey anti-mouse whole IgG-Alexa Fluor 488, 715-545-150, donkey anti-mouse whole IgG-Alexa Fluor 647, 715-605-150, donkey anti-rabbit whole IgG-Alexa Fluor 488, 711-545-152, donkey anti-rabbit whole IgG-Cy3, 711-166-152, donkey anti-goat whole IgG-Alexa Fluor 488, donkey anti-goat whole IgG-Cy3, 705-165-147, donkey anti-goat whole IgG-Alexa Fluor 647, 705-605-147, all from Jackson ImmunoResearch.

After blocking, all the triple, double or single staining (except “d25 Nkx2.1 (mouse)/ p63(rabbit)/FOXA2(goat)” and “Tuj1/TTF-1/FOXA2”) were performed by incubating primary antibody(ies), according to the dilution factors indicated in supplementary table I in staining/wash buffer (5% fetal donkey serum in PBS) at 4°C overnight (minimum 12hr), followed by 3×10min wash. The cultures were then incubated with the corresponding secondary antibodies at 1:300 dilutions in staining/wash buffer at room temperature for 2hr, washed twice for 10 min and incubated with DAPI for 5 min at room temperature. The stained cultures can be preserved in antibiotics supplemented PBS in dark at 4°C for 2–3 months. The d48 Mucin2, CC-10 SPB and pro-SPC can be preserved up to 6 months or longer. For better maintenance, we preserved the cultures in VECTASHIELD Mounting Media (Vector laboratories, Inc. Burlingame, CA, Cat# H-1000).

Samples were visualized and imaged using motorized Leica DMI 6000B fluorescence microscope coupled with Leica DFC365 FX digital camera and operated by LAS AF 6.2 software (Leica Microsystems GmbH, Wetzlar, Germany). All the pictures were imaged with HCX PL S-APO 10×/NA 0.3 or HCX PL FL L 20×/NA 0.4 objectives. The tile scan

images were taken with the image tiling module coupled with either autofocus or z-stack scanning (1.5μm/stack) module; and auto-stitched by the LAS AF 6.2 software. The images were exported as JPG files and processed (contrast and brightness adjustments) with Photoshop CS5.1 (New York, NY).

Mice and kidney capsule transplantation

NSG (NOD/SCID*Il2rg*−/−) mice purchased from The Jackson Laboratory (Bar Harbor, ME) were kept in a specific pathogen-free mouse facility and used at 8–12 weeks of age. Experiments were performed in accordance with the protocols approved by The Columbia University Institutional Animal Care And Use Committee. About one million of day15 lung progenitor cells were implanted under the kidney capsule. The outgrowths were excised at 2 and 6 months post transplantation. Outgrowths were embedded in OCT for immunofluorescence as described above, or fixed with 10% formalin and then processed for paraffin section and hematoxylin and eosin (H&E) stains to visualize the morphology. Samples were visualized and imaged using motorized Leica DMI 6000B fluorescence microscope as described above. H&E stains were visualized with the same microscope coupled with Leica DFC450 digital camera; the pictures were imaged with HCX PL FLUOTAR 5x/0.15, HC PLAN APO 20x/0.70, or HCX PL APO 100x/1.4-0.70 oil objectives.

Cell cultivation on decellularized slices of human lung

Human lungs rejected for transplantation were procured from the New York Organ Donor Network (NYODN) under a protocol approved by the Institutional Review Board at Columbia University. The lower left lobes of the lungs were sectioned to 2mm-thick sheets that were decellularized using our previously described method with 16mM 3-[(3-Cholamidopropyl) dimethylammonio]-1-propanesulfonate (CHAPS)[48]. This method effectively removed all cellular material while preserving the structure, mechanical properties and much of the molecular composition of the native lung matrix[48]. Decellularized lung slices were cored into 7 mm discs using a dermal punch and attached by fibrin to the wells in 96-well plates. All procedures were done under sterile conditions. Prior to cell seeding, the lung matrix was incubated in SFD medium for 48 hr to test sterility. Day 15 lung progenitors were replated after brief trypsinization onto the lung matrix at 1:5 dilution. Cultures on the lung matrix were maintained under conditions identical to those of fibronectin-coated cultures. At d48, the cultures on the matrix were embedded in OCT and processed for immunofluorescence of specific antigens as described above, or processed for live imaging of fluorescent-SPB protein localization as described below.

Quantitative Real-Time PCR

Total RNA was extracted using Trizol (Invitrogen), phase lock tubes (5′ Prime) and RNeasy kit (Qiagen, Valencia, CA). RNA concentration was measured with a NanoDrop 2000 fluorospectrometer (Thermo Fisher Scientific). RNA quality was verified using an Agilent microfluidic RNA 6000 Nano Chip kit on the 2100 Bioanalyzer (Agilent Technologies, Santa Clara, CA). cDNA was generated by reverse transcription of a total of 1μg RNA with random hexamers and Superscript III [Invitrogen (Life Technologies)]) following the

manufacturer's instructions. The reaction was carried out in a 20μL volume. Real-time quantitative PCR was performed on ABI vii7A Thermocycler [Applied Biosystems (Life Technologies)] using ABI Power SYBR Green PCR Master Mix [Applied Biosystems (Life Technologies)]. The Real-time PCR conditions were 50°C for 2 min and 95°C for 10 min followed by 40 cycles of 95 °C for 15 s and 60 °C for 1 min, dissociation/melt curves were obtained for each of the genes. Absolute quantification of each gene was obtained using a standard curve of serial diluted genomic DNA and normalized to housekeeping genes β-*ACTIN and TBP* (Tata Box Binding protein). Quantitative PCR for each sample were performed in triplicates, the input of template per triplicate was cDNA transcribed from 5–10ng of RNA. Primer sequences are listed in supplementary table II.

Live cell imaging of fluorescent-SPB protein localization in d48 cultures

D15 and 48 differentiation cultures on fibronectin-coated plates or decellularized human lung matrix were loaded with 8μg/ml purified, fluorescent human SPB (BODIPY-SPB) protein in SFD media, and incubated in a 5% CO2/air environment for 1 hr. Cultures were rinsed twice with SFD. Cultures on fibronectin-coated plates were imaged on motorized Leica DMI 6000B fluorescence microscope with HCX PL FL L 20X/NA 0.4 objective. Cultures on decellularized human lung matrix were imaged by laser scanning confocal microscope (LSM 510, Carl Zeiss Microscopy) using a 40X water immersion objective (numerical aperture 0.80).

Flow Cytometry

Day 4, 4.5 or 5 embryoid bodies were dissociated into single cells with 0.05% trypsin/EDTA. The cells were stained directly with PE conjugated CXCR4 (Invitrogen) (1:200), and APC conjugated c-KIT (BD Biosciences, San Jose, CA) (1:100) in PBS supplemented with 0.1% BSA and 0.2 mM EDTA for 45 min at 4°C. Stained cells were analzyed on a LSRII (BD Biosciences) and results were analyzed by Flowjo software (Tree Star, Ashland, OR).

For quantification of ATII cells in differentiated culture, day15 and d48 cultures were incubated with BODIPY-SPB for 1 hr as described above, in the presence of 10ng/ml Hoechst 33342 (Sigma). Cultures were rinsed with DPBS, trypsinized (0.05%) for 2 min at 37°C and passed through a 40 μM cell strainer. The single cell suspensions were stained with APC conjugated EpCAM in PBS supplemented with 0.1% BSA and 0.2 mM EDTA for 45 min at 4°C. Stained cells were analyzed on a LSRII (BD Biosciences) and results were analyzed by Flowjo software (Tree Star, Ashland, OR).

Electron Microscopy

D15 and d48 differentiation cultures and human fetal lung cultures grown on 35mm dishes (Thermo Fisher Scientific (Nunc), cat#153066) were fixed with 2.5% glutaraldehyde in 0.1M Sorensen's buffer for 2hr at room temperature. Samples were further processed, sectioned and stained by Columbia University Dept. of Pathology and Cell Biology Electron Microscope Facility. Sections were examined under a JEOL JEM-1200EXII electron microscope. Images were acquired on an ORCA-HR digital camera (Hamamatsu) and recorded with an AMT Image Capture Engin.

Statistical Analysis

Statistical analysis was performed using unpaired two-tailed student's *t*-test. For multiple group comparison (more than two), results were analyzed using one-way analysis of variance followed by Dunnett's multiple comparison test. Results were shown as Mean ± SEM, *p-Values* < 0.05 were considered statistically significant. Variances in all groups compared were similar.

For animal studies, no randomization was required. The investigator was not blinded to any group allocation. Animals showing signs of distress (weight loss >20%, inactivity, ruffled fur) are in principle euthanized. This did not occur in this study.

Supplementary Material

Refer to Web version on PubMed Central for supplementary material.

Acknowledgments

SXLH is a Druckenmiller Fellow of the New York Stem Cell Foundation. The authors wish to thank Dr. Josh Sonnet and the Columbia Lung Regeneration Team, Dr. Donna Farber and Mr. Joseph Thome for providing samples of human lung tissue; Ms. Kristy Brown for kind help with Electron Microscopy; Dr. Siu-Hong Ho for assistance with Microscopy.

References

1. Green MD, Huang SX, Snoeck HW. Stem cells of the respiratory system: From identification to differentiation into functional epithelium. BioEssays: news and reviews in molecular, cellular and developmental biology. 2012
2. Rock JR, Hogan BL. Epithelial progenitor cells in lung development, maintenance, repair, and disease. Annu Rev Cell Dev Biol. 2011; 27:493–512. [PubMed: 21639799]
3. Morrisey EE, Hogan BL. Preparing for the first breath: genetic and cellular mechanisms in lung development. Dev Cell. 2010; 18:8–23. [PubMed: 20152174]
4. Rawlins EL, Clark CP, Xue Y, Hogan BL. The Id2+ distal tip lung epithelium contains individual multipotent embryonic progenitor cells. Development. 2009; 136:3741–3745. [PubMed: 19855016]
5. Green MD, et al. Generation of anterior foregut endoderm from human embryonic and induced pluripotent stem cells. Nature biotechnology. 2011; 29:267–272.
6. Mou H, et al. Generation of Multipotent Lung and Airway Progenitors from Mouse ESCs and Patient-Specific Cystic Fibrosis iPSCs. Cell Stem Cell. 2012; 10:385–397. [PubMed: 22482504]
7. Longmire TA, et al. Efficient derivation of purified lung and thyroid progenitors from embryonic stem cells. Cell Stem Cell. 2012; 10:398–411. [PubMed: 22482505]
8. Wong AP, et al. Directed differentiation of human pluripotent stem cells into mature airway epithelia expressing functional CFTRTR protein. Nature biotechnology. 2012; 30:876–882.
9. Kubo A, et al. Development of definitive endoderm from embryonic stem cells in culture. Development. 2004; 131:1651–1662. [PubMed: 14998924]
10. Nostro MC, Keller G. Generation of beta cells from human pluripotent stem cells: Potential for regenerative medicine. Seminars in cell & developmental biology. 2012
11. Nostro MC, et al. Stage-specific signaling through TGFbeta family members and WNT regulates patterning and pancreatic specification of human pluripotent stem cells. Development. 2011; 138:861–871. [PubMed: 21270052]
12. D'Amour KA, et al. Efficient differentiation of human embryonic stem cells to definitive endoderm. Nature biotechnology. 2005; 23:1534–1541.
13. Goss AM, et al. Wnt2/2b and beta-catenin signaling are necessary and sufficient to specify lung progenitors in the foregut. Dev Cell. 2009; 17:290–298. [PubMed: 19686689]

14. Bellusci S, Grindley J, Emoto H, Itoh N, Hogan BL. Fibroblast growth factor 10 (FGF10) and branching morphogenesis in the embryonic mouse lung. Development. 1997; 124:4867–4878. [PubMed: 9428423]
15. Bellusci S, Henderson R, Winnier G, Oikawa T, Hogan BL. Evidence from normal expression and targeted misexpression that bone morphogenetic protein (Bmp-4) plays a role in mouse embryonic lung morphogenesis. Development. 1996; 122:1693–1702. [PubMed: 8674409]
16. Domyan ET, et al. Signaling through BMP receptors promotes respiratory identity in the foregut via repression of Sox2. Development. 2011; 138:971–981. [PubMed: 21303850]
17. Li Y, Gordon J, Manley NR, Litingtung Y, Chiang C. Bmp4 is required for tracheal formation: a novel mouse model for tracheal agenesis. Developmental biology. 2008; 322:145–155. [PubMed: 18692041]
18. Chen F, et al. A retinoic acid-dependent network in the foregut controls formation of the mouse lung primordium. J Clin Invest. 2010; 120:2040–2048. [PubMed: 20484817]
19. Yamamoto M, et al. Nodal antagonists regulate formation of the anteroposterior axis of the mouse embryo. Nature. 2004; 428:387–392. [PubMed: 15004567]
20. Perea-Gomez A, et al. Nodal antagonists in the anterior visceral endoderm prevent the formation of multiple primitive streaks. Dev Cell. 2002; 3:745–756. [PubMed: 12431380]
21. del Barco Barrantes I, Davidson G, Grone HJ, Westphal H, Niehrs C. Dkk1 and noggin cooperate in mammalian head induction. Genes Dev. 2003; 17:2239–2244. [PubMed: 12952897]
22. Yu PB, et al. Dorsomorphin inhibits BMP signals required for embryogenesis and iron metabolism. Nature chemical biology. 2008; 4:33–41. [PubMed: 18026094]
23. Inman GJ, et al. SB-431542 is a potent and specific inhibitor of transforming growth factor-beta superfamily type I activin receptor-like kinase (ALK) receptors ALK4, ALK5, and ALK7. Molecular pharmacology. 2002; 62:65–74. [PubMed: 12065756]
24. Chen B, et al. Small molecule-mediated disruption of Wnt-dependent signaling in tissue regeneration and cancer. Nature chemical biology. 2009; 5:100–107. [PubMed: 19125156]
25. Bennett CN, et al. Regulation of Wnt signaling during adipogenesis. The Journal of biological chemistry. 2002; 277:30998–31004. [PubMed: 12055200]
26. Fusaki N, Ban H, Nishiyama A, Saeki K, Hasegawa M. Efficient induction of transgene-free human pluripotent stem cells using a vector based on Sendai virus, an RNA virus that does not integrate into the host genome. Proceedings of the Japan Academy. Series B, Physical and biological sciences. 2009; 85:348–362.
27. Warren L, et al. Highly efficient reprogramming to pluripotency and directed differentiation of human cells with synthetic modified mRNA. Cell Stem Cell. 2010; 7:618–630. [PubMed: 20888316]
28. Kimura S, et al. The T/ebp null mouse: thyroid-specific enhancer-binding protein is essential for the organogenesis of the thyroid, lung, ventral forebrain, and pituitary. Genes Dev. 1996; 10:60–69. [PubMed: 8557195]
29. Kriks S, et al. Dopamine neurons derived from human ES cells efficiently engraft in animal models of Parkinson's disease. Nature. 2011; 480:547–551. [PubMed: 22056989]
30. Harris-Johnson KS, Domyan ET, Vezina CM, Sun X. beta-Catenin promotes respiratory progenitor identity in mouse foregut. Proc Natl Acad Sci U S A. 2009; 106:16287–16292. [PubMed: 19805295]
31. Rock JR, et al. Basal cells as stem cells of the mouse trachea and human airway epithelium. Proc Natl Acad Sci U S A. 2009; 106:12771–12775. [PubMed: 19625615]
32. Weaver M, Yingling JM, Dunn NR, Bellusci S, Hogan BL. Bmp signaling regulates proximal-distal differentiation of endoderm in mouse lung development. Development. 1999; 126:4005–4015. [PubMed: 10457010]
33. Shu W, et al. Wnt/beta-catenin signaling acts upstream of N-myc, BMP4, and FGF signaling to regulate proximal-distal patterning in the lung. Developmental biology. 2005; 283:226–239. [PubMed: 15907834]
34. Post M, et al. Keratinocyte growth factor and its receptor are involved in regulating early lung branching. Development. 1996; 122:3107–3115. [PubMed: 8898224]

35. Malpel S, Mendelsohn C, Cardoso WV. Regulation of retinoic acid signaling during lung morphogenesis. Development. 2000; 127:3057–3067. [PubMed: 10862743]
36. Wongtrakool C, et al. Down-regulation of retinoic acid receptor alpha signaling is required for sacculation and type I cell formation in the developing lung. The Journal of biological chemistry. 2003; 278:46911–46918. [PubMed: 12947094]
37. Gonzales LW, Guttentag SH, Wade KC, Postle AD, Ballard PL. Differentiation of human pulmonary type II cells in vitro by glucocorticoid plus cAMP. American journal of physiology. Lung cellular and molecular physiology. 2002; 283:L940–951. [PubMed: 12376347]
38. Sanchez-Esteban J, et al. Mechanical stretch promotes alveolar epithelial type II cell differentiation. J Appl Physiol. 2001; 91:589–595. [PubMed: 11457769]
39. Whitsett JA, Wert SE, Weaver TE. Alveolar surfactant homeostasis and the pathogenesis of pulmonary disease. Annual review of medicine. 2010; 61:105–119.
40. Rooney SA. Regulation of surfactant secretion. Comparative biochemistry and physiology. Part A, Molecular & integrative physiology. 2001; 129:233–243.
41. Gouon-Evans V, et al. BMP-4 is required for hepatic specification of mouse embryonic stem cell-derived definitive endoderm. Nature biotechnology. 2006; 24:1402–1411.
42. Osafune K, et al. Marked differences in differentiation propensity among human embryonic stem cell lines. Nature biotechnology. 2008; 26:313–315.
43. Bock C, et al. Reference Maps of human ES and iPS cell variation enable high-throughput characterization of pluripotent cell lines. Cell. 2011; 144:439–452. [PubMed: 21295703]
44. Boulting GL, et al. A functionally characterized test set of human induced pluripotent stem cells. Nature biotechnology. 2011; 29:279–286.
45. Blauwkamp TA, Nigam S, Ardehali R, Weissman IL, Nusse R. Endogenous Wnt signalling in human embryonic stem cells generates an equilibrium of distinct lineage-specified progenitors. Nature communications. 2012; 3:1070.
46. Barkauskas CE, et al. Type 2 alveolar cells are stem cells in adult lung. J Clin Invest. 2013
47. Xu X, et al. Evidence for type II cells as cells of origin of K-Ras-induced distal lung adenocarcinoma. Proc Natl Acad Sci U S A. 2012; 109:4910–4915. [PubMed: 22411819]
48. O'Neill JD, et al. Decellularization of Human and Porcine Lung Tissues for Pulmonary Tissue Engineering. The Annals of thoracic surgery. 2013

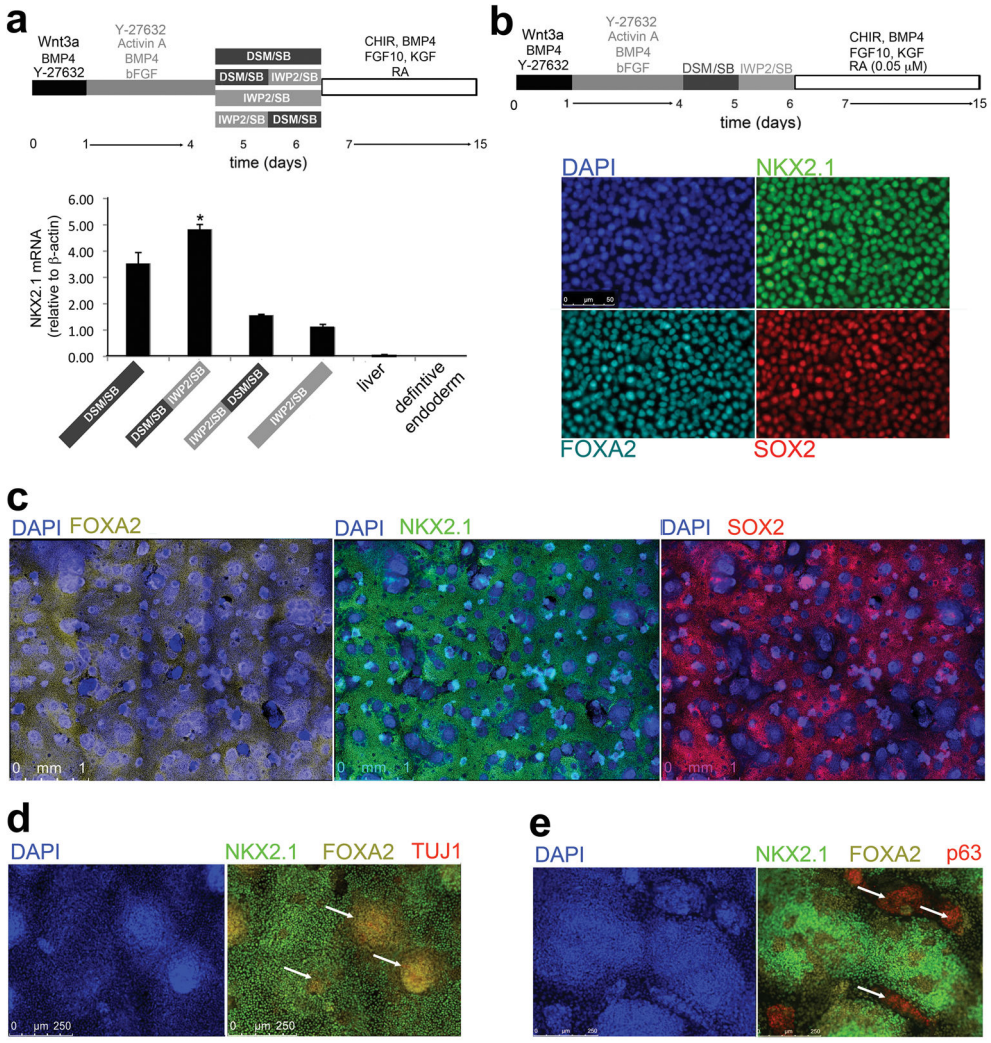

Fig. 1. Establishment of a protocol of lung field induction

(a) Expression of NKX2.1 mRNA at d15 in the four culture conditions shown on top of the panel. **P*<0.01, compared with IWP2/SB->DSM/SB group, triplicate experiments. 'Liver' represents DE cultured in 'hepatic conditions'[41], data for definitive endoderm are samples analyzed at d4.5 of the differentiation protocol. **(b)** Expression of FOXA2, SOX2 and NKX2.1 in RUES2 cells cultured according to the protocol on top of the panel. **(c)** 10x tile scan of 25 (5×5) contiguous fields showing expression of FOXA2, SOX2 and NKX2.1 in RUES2 cells cultured according to the protocol on top of panel **(b)**. **(d)** 20x tile scan of 4 (2×2) contiguous fields showing expression of TUJ1, NKX2.1 and FOXA2.1 in RUES2 cells cultured according to the protocol on top of panel (b**). (e)** 20x tile scan of 4 (2×2) contiguous fields showing expression of p63, NKX2.1 and FOXA2.1 in RUES2 cells cultured according to the protocol on top of panel (b**).** Immunofluorescence images from Fig. 2a–d represent reproducible results from 3 independent experiments.

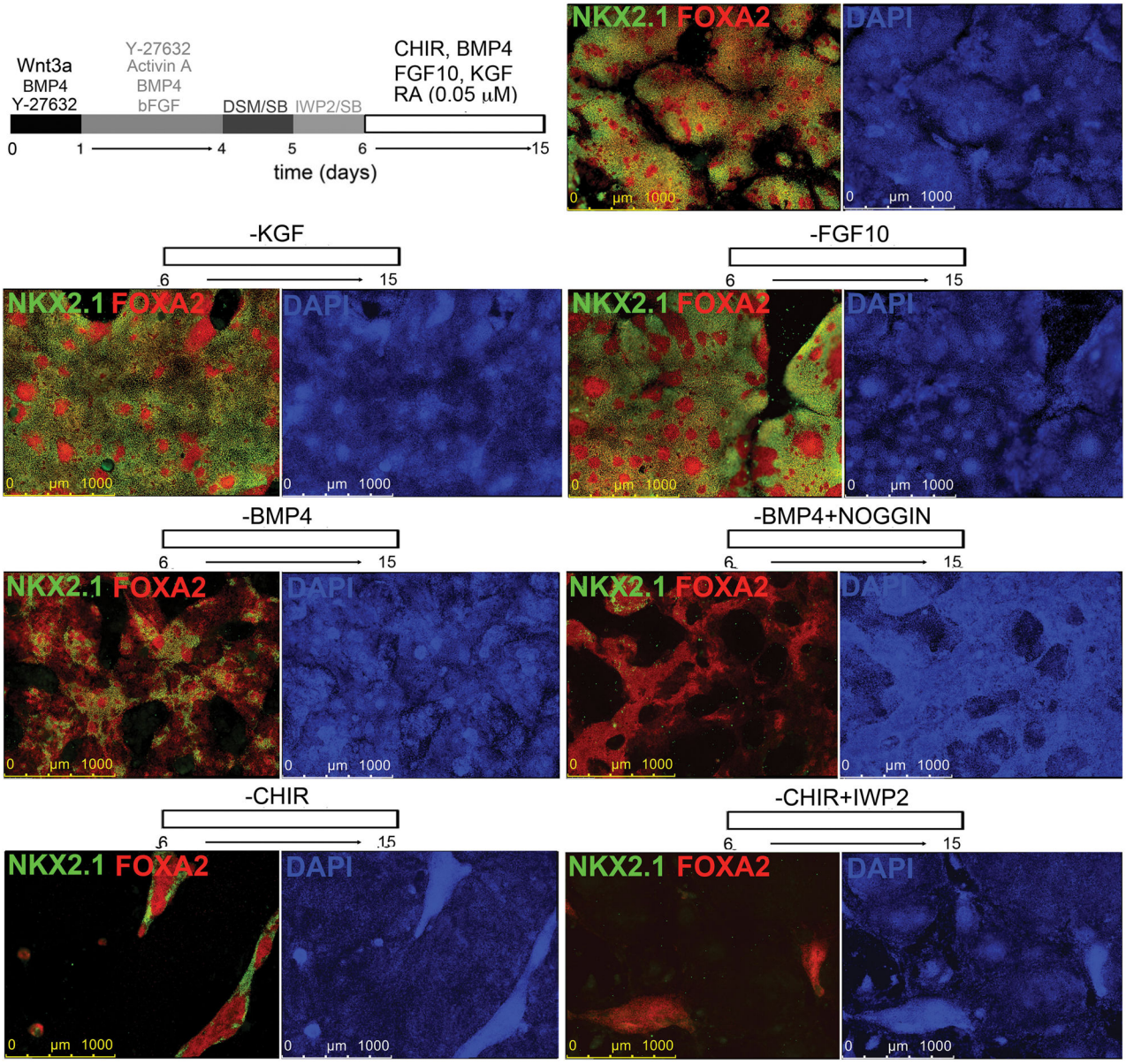

Fig. 2. Requirement of morphogens for lung field induction from hPSCs

Effect of removing individual factors or blocking signaling pathways during the 'ventralization' stage (d6–d15) on the expression of FOXA2 and NKX2.1 in RUES2 cells cultured according to the protocol shown on the upper left of the figure. 10x tile scans of 9 (3×3) contiguous fields. Immunofluorescence images represent reproducible results from 3 independent experiments.

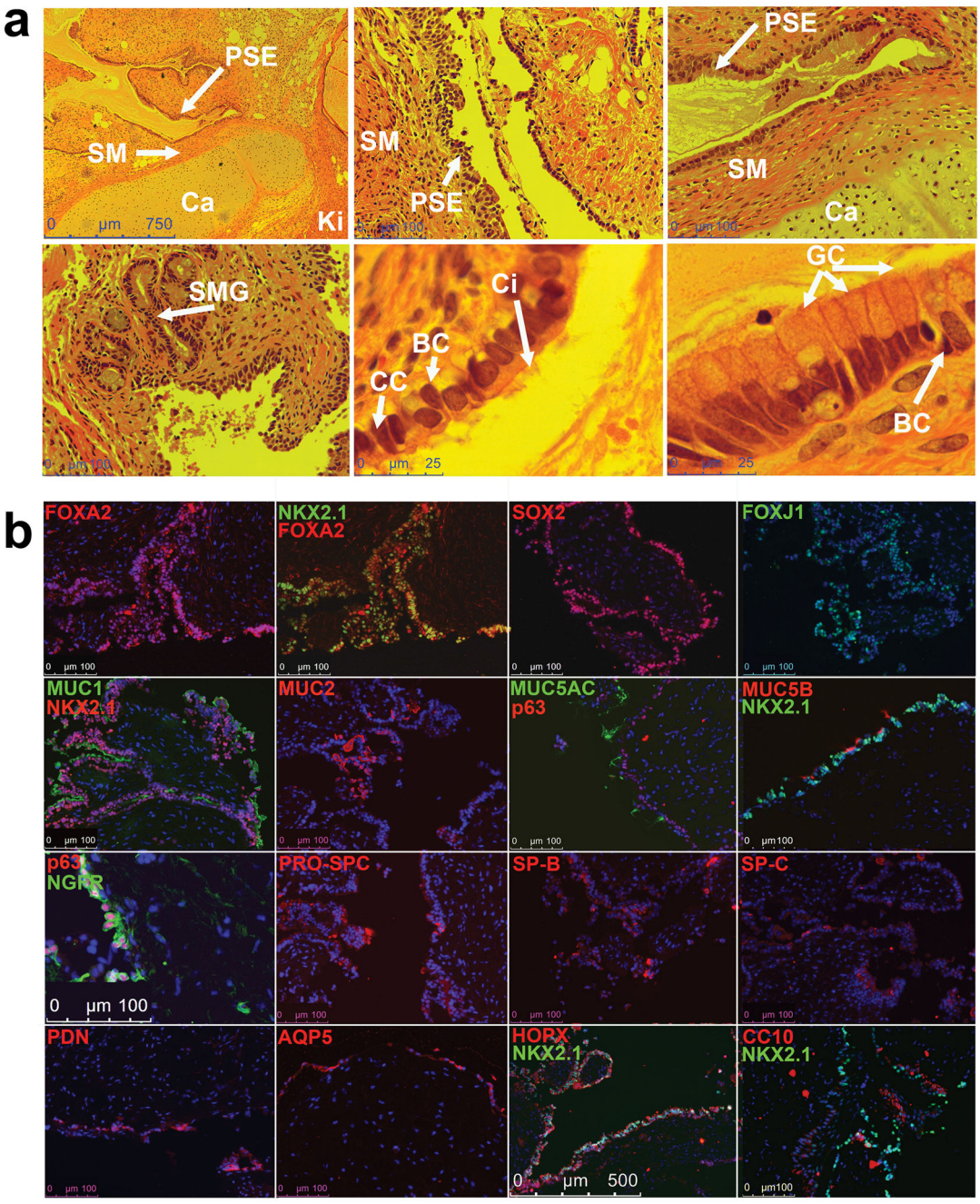

Fig. 3. *In vivo* potential of hPSC-derived lung and airway progenitors

(a) Representative examples of H&E stains of growths removed 6 months after transplantation of RUES2 cells differentiated according to the protocol shown in Fig. 1b, under the kidney capsule of NSG mice (BC: basal cell; Ca: cartilage; CC: Clara cell; Ci: ciliated cell; GC: goblet cell; Ki: mouse kidney; PSE: pseudostratified epithelium; SM: smooth muscle; SMG: submucosal glands). **(b)** Representative examples of the expression of markers of mature lung and airway epithelial cells in the growths from **(a).** Representative of 4 animals.

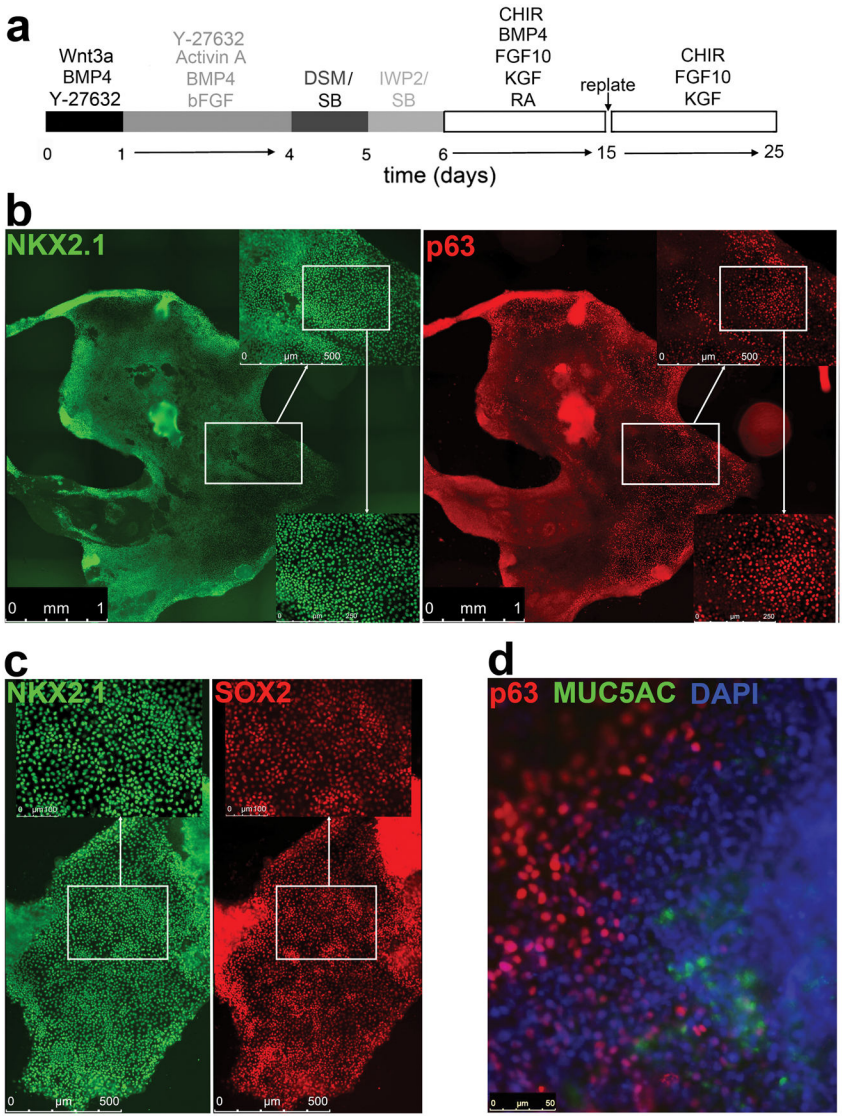

Fig. 4. Further differentiation of hPSCS-derived lung and airway progenitors

(a) Culture protocol of RUES2 cells shown in panels (b), (c) and (d). **(b)** and **(c)** 10x tile scans of the expression of p63, SOX2 and NKX2.1 in representative colonies obtained after culturing RUES2 cells according to the protocol shown in (a). **(d)** Expression of p63 and MUC5AC after culturing RUES2 cells according to the protocol shown in panel (a). Immunofluorescence images represent reproducible results from 4 independent experiments.

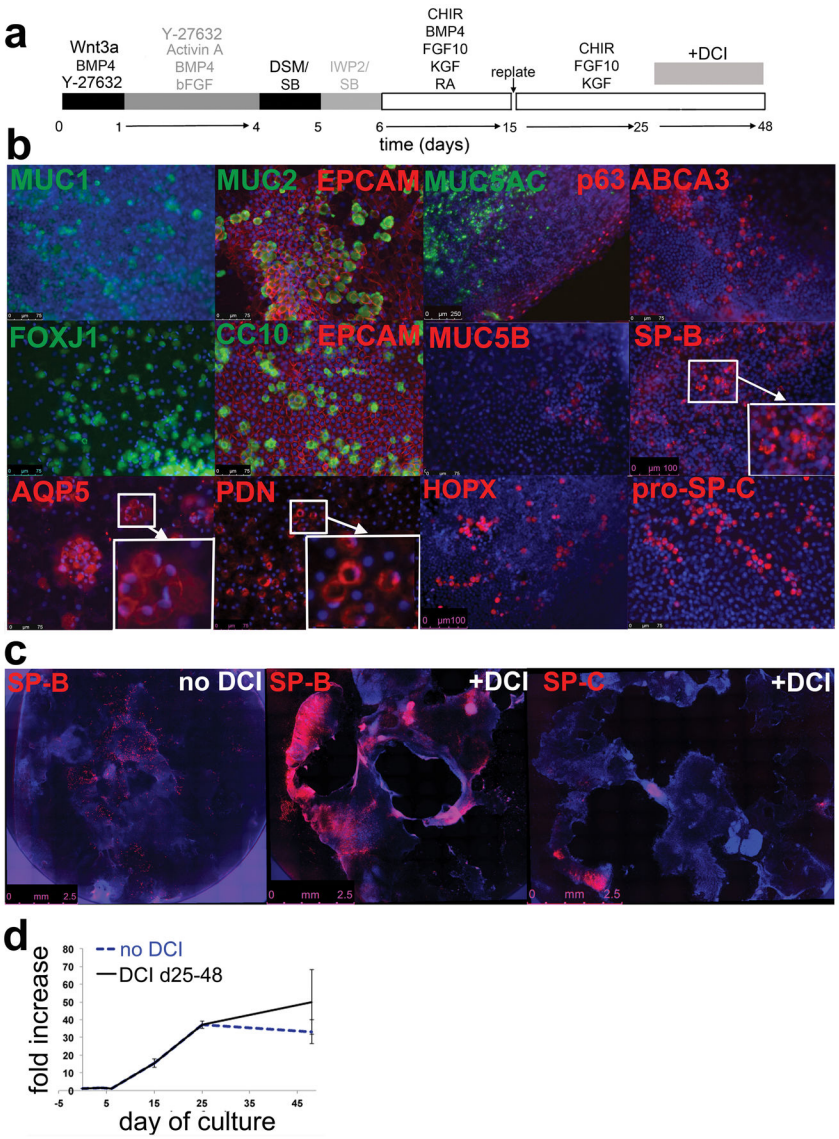

Fig. 5. Terminal differentiation of hPSCS-derived lung and airway progenitors

(a) Culture protocol of RUES2 cells shown in panels (b), (c) and (d). **(b)** Representative examples of the expression of markers of mature lung and airway epithelial cells after culturing RUES2 cells according to the protocol shown in panel (a). Immunofluorescence images represent reproducible results from 4 independent experiments. **(c)** Representative 10x whole culture tile scan of SP-B and SP-C expression in RUES2 cells cultured according to the protocol shown in (a), without (left) and with (right) addition of DCI at d25. **(d)** Cellular expansion of RUES2 cells during the culture according to the protocol shown on top of panel (a) (n=4).

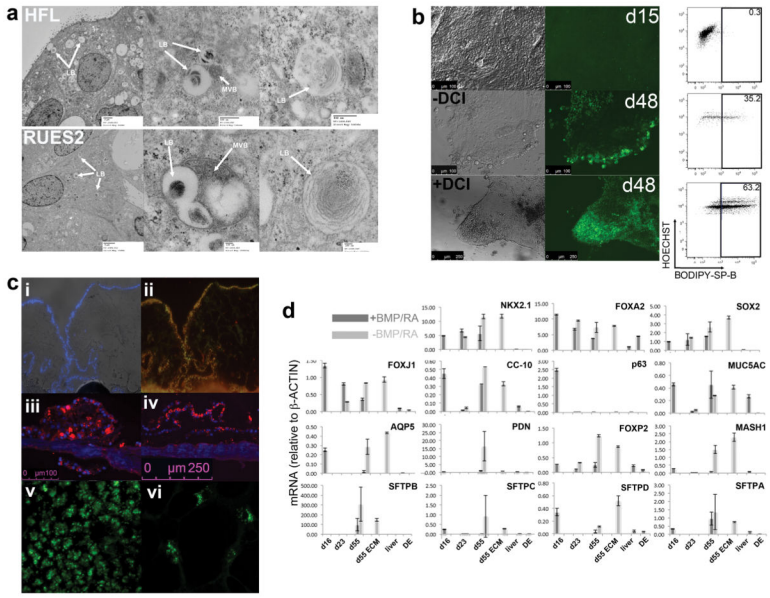

Fig. 6. Morphology and function of hPSC-derived lung and airway epithelium

(a) Representative transmission electron micrographs of cultured FHL or RUES2 cells differentiated according to the protocol shown in Fig. 5a with DCI (LB: lamellar body; MVB: mulitvesicular body) **(b).** Fluorescence micrographs and flow cytometric analysis of **u**ptake of BODIPY-SP-B by cells cultured according to the protocol shown in Fig. 5 a. Immunofluorescence images and flow cytometry represent reproducible results from 3 independent experiments. **(c)** Culture in the presence of decellularized human lung matrix. *(i and ii)* Expression p63 and NKX2.1 at d25 of cultures of RUES2 cells seeded on slices of decellularized human lung matrix at day 15 of the protocol in Fig. 5a. *(iii and iv)* Expression of endogenous SP-B at d48 of culture with DCI according to the protocol in Fig. 5a after seeded on decellularized human lung matrix *(v)* Confocal fluorescence micrograph of the uptake of BODIPY-SP-B at d48 in the same conditions *(vi)* Morphology of mouse ATII cells as observed by two-photon microscopy of live mouse lung after instillation of BODIPY-SPB. **(d)** qPCR of the expression of proximal and distal lung markers at days 15, 23 and 55 of culture in the conditions in Fig. 5a in the presence of DCI. Cultures in the presence or absence of BMP4 and RA (+BMP/RA vs. –BMP/RA) from d15 to d55 were compared. (ECM = human decellularized extracellular lung matrix) (representative triplicate experiment).